

13. H. Rabitz *et al.*, *Science* **288**, 824 (2000).  
 14. H. Rabitz, W. S. Zhu, *Acc. Chem. Res.* **33**, 572 (2000).  
 15. R. J. Levis, M. J. DeWitt, *J. Phys. Chem. A* **103**, 6493 (1999).  
 16. J. M. Geremia, W. S. Zhu, H. Rabitz, *J. Chem. Phys.* **113**, 10841 (2000).  
 17. M. M. Wefers, K. A. Nelson, *J. Opt. Soc. Am. B* **12**, 1343 (1995).  
 18. D. Goldberg, *Genetic Algorithms in Search Optimization and Machine Learning* (Addison-Wesley, Reading, MA, 1989).  
 19. M. Demiralp, H. Rabitz, *Phys. Rev. A* **47**, 809 (1993).  
 20. K. Sundermann, H. Rabitz, R. de Vivie-Riedle, *Phys. Rev. A* **62**, 013409 (2000) (available at <http://link.aps.org/abstract/PRA/v62/e013409>).  
 21. In the reference experiments, the intensity of the

laser pulse was decreased by inserting glass coverslips into the beam before focusing, which decreased the intensity by  $\sim 7\%$  per slide. The pulse duration was increased by placing a linear chirp on the pulse by either increasing or decreasing the position of the second grating in the compressor. The mass spectra were recorded and analyzed as a function of these two variables to provide a reference for the shaped-pulse control experiments.  
 22. M. J. DeWitt, R. J. Levis, *J. Chem. Phys.* **110**, 11368 (1999).  
 23. R. J. Levis, G. M. Menkir, H. Rabitz, data not shown.  
 24. Drawing unambiguous mechanistic conclusions from analysis of the detailed kinematic field structures alone is difficult at this time. Furthermore, before analyzing the field, suitable cost functions need to be

introduced in the algorithm guiding the experiments to assure that only the essential structure is retained (16).  
 25. J. Berkowitz, G. B. Ellison, D. Gutman, *J. Chem. Phys.* **98**, 2744 (1994).  
 26. The authors acknowledge the support of the Office of Naval Research, the Army Research Office, the NSF, and the Sloan and Dreyfus foundations for the support of this research. R.J.L. acknowledges fruitful discussions with A. Markevitch, N. P. Moore, and P. Graham.

18 January 2001; accepted 15 March 2001

Published online 29 March 2001;  
 10.1126/science.1059133

Include this information when citing this paper.

## A Complex Pattern of Mantle Flow in the Lau Backarc

Gideon P. Smith,<sup>1</sup> Douglas A. Wiens,<sup>1</sup> Karen M. Fischer,<sup>2</sup> Leroy M. Dorman,<sup>3</sup> Spahr C. Webb,<sup>4</sup> John A. Hildebrand<sup>3</sup>

Shear-wave splitting analysis of local events recorded on land and on the ocean floor in the Tonga arc and Lau backarc indicate a complex pattern of azimuthal anisotropy that cannot be explained by mantle flow coupled to the downgoing plate. These observations suggest that the direction of mantle flow rotates from convergence-parallel in the Fiji plateau to north-south beneath the Lau basin and arc-parallel beneath the Tonga arc. These results correlate with helium isotopes that map mantle flow of the Samoan plume into the Lau basin through an opening tear in the Pacific plate.

Seismic anisotropy ( $I$ ) is usually attributed to the alignment of crystal orientations, which in turn can be related to the strain history of the rock (2–5). Strain can also be inferred from modeling of mantle flow (6), and thus observation of seismic anisotropy can be used to map mantle flow at length scales related to the wavelength of the seismic waves. Many observations of anisotropy have been made in the region of subduction zones (7). However, an unambiguous interpretation of these results is often difficult because of poor station coverage or nonuniform source distribution. Here we use a unique data set, which spans an active backarc basin and spreading center, to map out the mantle flow in a backarc system and compare the seismic measurements to geochemical studies and model predictions.

Modeling of the strain resulting from flow coupled to the subducting plate (6, 8) predicts a fairly uniform pattern of anisotropy, with a fast direction parallel to the absolute plate motion of the downgoing plate. A variety of shear-wave ( $S$ -wave) splitting measurements

at island stations in backarc areas are consistent with this pattern (9–14) or with flow coupled to both subducting and overlying plates. However, closer to the trench and slab, the pattern of mantle flow may become more complex. Large-scale deviation of mantle flow due to retrograde motion of the subducted slab has been postulated (15) and was reported by  $S$ -wave splitting studies in South America (16). Similar observations in New Zealand (17) and Kamchatka (18) may also result from such a flow pattern. Physical modeling of subduction zone flow also indicates strong variations in mineral alignment with slab dip (19). Numerical modeling of the likely induced lattice preferred orientation of olivine and orthopyroxene produces results that are non-unique and may only be fully tested with a more detailed mapping of the backarc system (13, 20). It is often difficult to infer the exact location of the anisotropy and thus to determine whether observations result from propagation within an anisotropic mantle wedge or within the slab.

In the Lau backarc, there is also the question of the effect of the small-scale processes associated with the spreading center. Although modeling predicts vertical preferential alignment of the olivine  $a$  axis due to the upwelling flow (21), a variety of fast directions have been noted in other spreading regions (22–26).

In this study, we present splitting mea-

surements from the Lau backarc. These observations provide strong constraints on lateral variations in the fast axis and thus allow us to distinguish geographic variations in anisotropy that may occur across the backarc basin. The region of the Lau basin and Tonga arc contains both an active backarc spreading center and a rapidly subducting slab (at a rate of 240 mm/year), so there should be a strong and variable signature of mantle flow. The high rate of seismic activity in this region also provides numerous high-energy sources for  $S$ -wave studies.

We analyzed  $S$ -wave splitting in arrivals from local earthquakes occurring beneath the Lau backarc. Data were obtained from the southwest Pacific seismic experiment (SPASE) and from the Lau basin ocean-bottom seismograph (OBS) survey (LaBatts). The SPASE array was deployed for 2 years and consisted of 12 broadband stations in Fiji, Tonga, and Niue Island. LaBatts was a concurrent 3-month deployment of 29 OBSs in the Lau backarc and Tonga forearc.

The OBS instrument orientations (27) were determined by comparing the polarization angles (28) of the  $P$  waves and Rayleigh waves from large, well-located, distant events, with known back azimuth. Splitting observations (29) were obtained using a cross-correlation of the two  $S$  waves calculated for a range of rotation angles,  $\varphi$ , and time offsets,  $\delta t$  (9). The  $\delta t$  and  $\varphi$  providing the maximum cross-correlation are the splitting time and fast anisotropy azimuth (Fig. 1). Some of the land station observations are taken from the analysis of Fischer and Wiens (10). Reanalysis of a subset of the Fischer and Wiens (10) data set using this method produced identical results, indicating that there is no bias between the results from the two studies. In order to avoid interference from the free surface or crustal phase conversions, we restricted our analysis to arrivals inside the  $S$ -wave “window” (incidence angles  $< 35^\circ$ ).

Well-constrained splitting parameters were obtained for 77 arrivals at the OBS stations and were combined with the existing 53 observations at land stations (10). Seventeen new land observations were also obtained at Kadavu Island and at land stations at

<sup>1</sup>Department of Earth and Planetary Sciences, Washington University in St. Louis, 1 Brookings Drive, CB1169, St. Louis, MO 63130, USA. <sup>2</sup>Department of Geological Sciences, Box 1846, Brown University, Providence, RI 02912, USA. <sup>3</sup>Scripps Institution of Oceanography, University of California, San Diego, La Jolla, CA 92093–0215, USA. <sup>4</sup>Lamont-Doherty Earth Observatory, Post Office Box 1000, 61 Route 9W, Palisades, NY 10964, USA.

REPORTS

the eastern end of the basin (Fig. 2). Results at the land-based stations on the Fiji platform to the west are consistent with the direction of subducting plate motion (10). However, the pattern of fast azimuths paralleling the subduction direction for stations on the Fiji plat-

form is not apparent for stations in the Lau basin and Tonga arc. Indeed, many of the fast vectors are almost trench parallel, perpendicular to the azimuth of Pacific plate motion, and the magnitude of the splitting varies with smaller splitting times near the spreading

center. This observation is not predicted by two-dimensional (2D) flow modeling, which instead predicts an almost uniform splitting time across the basin (20).

The splitting observations made for station LKBA indicate a variation in the observed splitting with source region (Fig. 3). Events in the northern part of the basin indicate a distinct north-south anisotropic fast direction (Fig. 3). This contrasts with the plate-motion-parallel directions in the southern and western part of the basin and is indicative of raypath dependence for the anisotropy. Neither variations at this length scale nor the fast direction rotation are predicted by mantle flow that is driven by simple coupling to the overlying or subducted plates, assuming uniform viscosity and an infinite planar slab (13).

For station NUKU (Fig. 4), most of the splitting observations are from intermediate-depth events (at depths of 150 to 300 km). Several of these are within 200 km of the station, and because of their relative location, they are unlikely to have significant path lengths within the slab. This indicates that the along-strike azimuthal observations should be explained by processes occurring within the mantle wedge and cannot be attributed to anisotropy within the subducted plate.

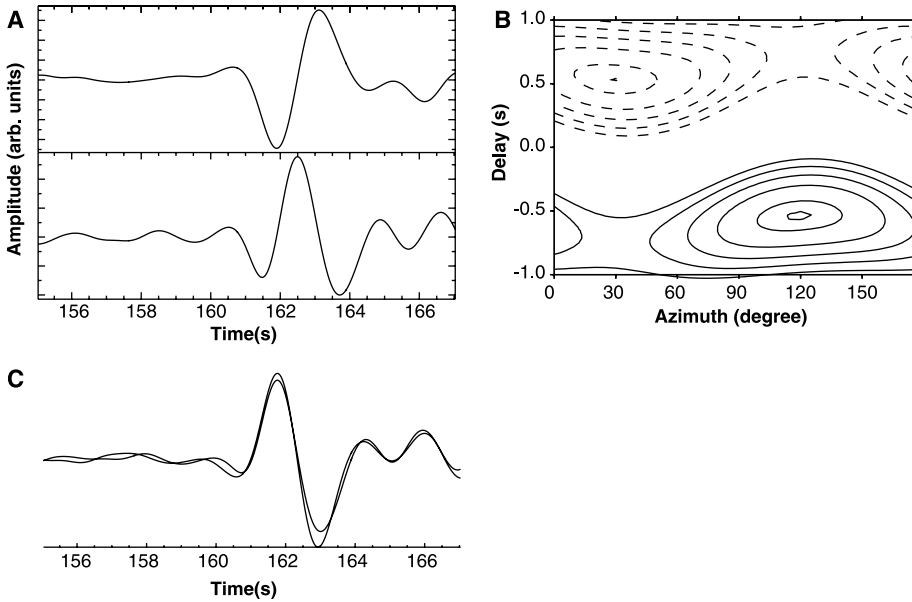


Fig. 1. (A) The original horizontal component seismograms recorded at OBS10. (B) Result of the cross-correlation. The correlation coefficient at different azimuths and delay times has been contoured, and a maximum was found at 120°, -0.5 s. (C) The final rotated and time-shifted seismograms.

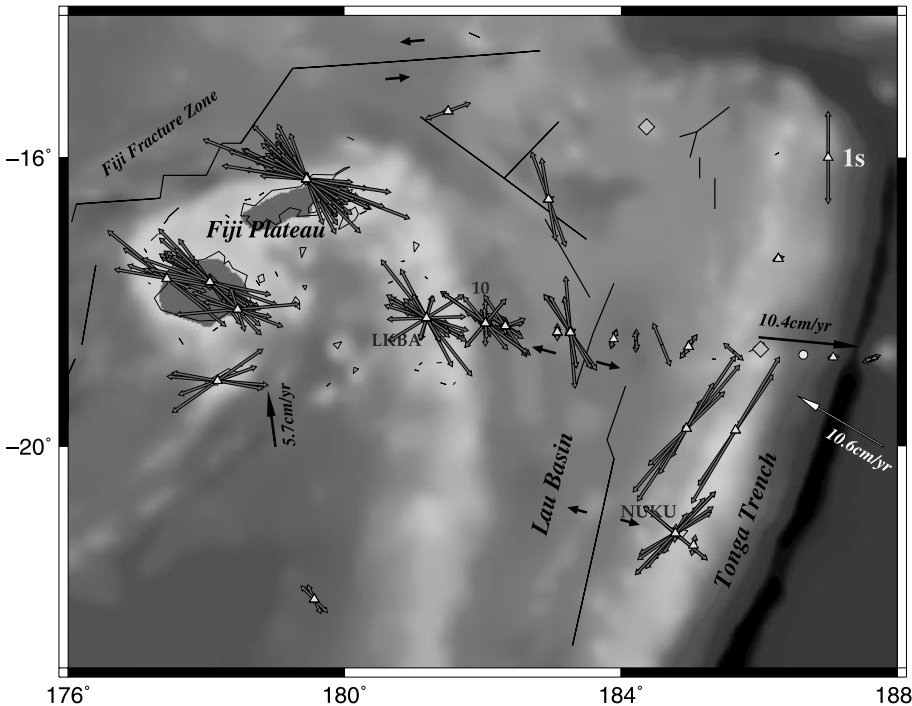


Fig. 2. Stations used in the current study (triangles). Splitting observations are plotted at the stations as vectors. The azimuth of each vector is the fast splitting direction, and its length is proportional to the splitting time. Stations LKBA, NUKU, and OBS10 are marked. Land stations where no well-constrained measurements were possible are marked with diamonds. The ocean-bottom station where null measurements were made is marked with a circle. The bold single-headed arrows indicate absolute plate motion vectors (39, 40).

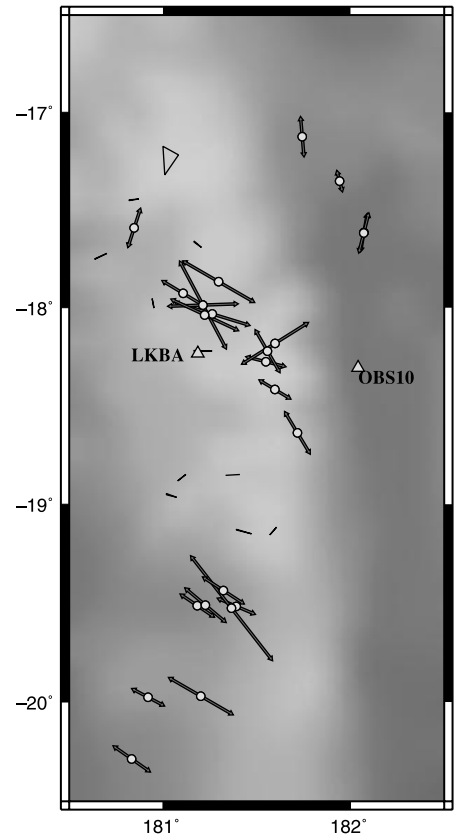


Fig. 3. Splitting observations made for station LKBA plotted as vectors at the midpoint between station and event locations. Stations are plotted as triangles.

## REPORTS

The observation of splitting fast axes parallel to the convergence direction at the western land stations (Fig. 2) can be explained by the large-scale deformation of the mantle driven by local coupling to the overlying and subducting plates. Fischer *et al.* (20) demonstrated that, given reasonable assumptions relating the strength of lattice preferred orientation to strain, the magnitude of the observed splitting times could also be predicted by plate-driven mantle flow models (13, 20).

Although this type of modeling works well for the stations at the western end of the basin, the large-scale mantle flow cannot reproduce either the source-region-dependent anisotropic variations (Fig. 3) or the direction and splitting times across the whole basin. To explain the trends in our data, we need to account for the structures in the backarc. Splitting times in the center of the basin are reduced and are almost orthogonal to the plate motion direction. Interpretation of this phenomenon as being related to the spreading center, which is geographically close, would fit qualitatively with the modeling of Blackman *et al.* (21). They used a finite element flow model to predict deformation in the vicinity of a spreading ridge. Elsewhere at mid-ocean ridges, surface waves have shown a similar pattern (26), although the rotation was not observed in SKS measurements, which possibly integrated this signature with the signature of deeper mantle flow (24). However, although the direction of anisotropy is consistently north to south, the magnitudes are highly variable from station to station, suggesting that this effect may not be due to processes on the length scale of the spreading center.

Closer to the trench, we measured large trench-parallel splitting. To explain these observations, we need to consider the presence of the subducting slab, because this is likely to be the dominant factor in determining the anisotropy close to the trench. Several explanations for the along-arc fast direction orientations must be considered. Water content may affect the deformation (30) and lattice preferred orientation of olivine (31) and thus may provide an explanation for the observations near the slab. However, the exact relationship between strain and anisotropy, and how the observations in the laboratory translate into observations in the real Earth, are still poorly understood, and preliminary laboratory results indicate that this mechanism would not produce the observed rotation (31). A second alternative is the anisotropic effect of thin melt sheets or pockets (32). 2D models of mantle flow predict melt sheet orientations that would produce a trench-parallel fast direction (20, 33). However, this interpretation is not entirely supported by the observations made of a progressively rotating anisotropic fast direction. In addition, neither explanation in terms of melt anisotropy nor the effect of

water content can explain the difference between our results in Tonga and those in the Marianas and Izu-Bonin. Previous studies show that both the Marianas (34) and Izu-Bonin (11) instead exhibit strong anisotropy perpendicular to the strike of the trench. If a generalized explanation were possible for the rotation of the fast direction in Tonga, such as either melt anisotropy or water content, it should also be observed in these other regions. Instead, we must appeal to the individual tectonics of the different regions to explain their measurements. One such possible hypothesis is that the absolute plate motions contain trench-parallel components that result in the lithosphere between the Lau spreading center and arc moving southward relative to the slab and the Australian plate. However, in uniform viscosity models for Tonga with an infinite planar slab, this produces an insufficient rotation of the fast directions

(13). We must also consider transpressional deformation in the overlying plate. This mechanism should produce compression parallel to convergence and thus alignment of olivine along the arc. However, this explanation is inconsistent with observations in various subduction zones that the anisotropy increases with depth. In addition, in Tonga we have rapid trench rollback, implying extension within the arc.

One possible explanation is the effect of slab rollback on mantle flow. The Tonga trench axis is moving eastward at an absolute velocity of  $\sim 10$  cm/year, and the dip of the Tonga slab has become progressively shallower over the past few million years. Buttles and Olson (19) examined the alignment of the olivine *a* axis using a laboratory analogy. They showed that the rollback component of plate motion can produce variations in mineral alignments. Their results indicated trench-parallel alignment in the

**Fig. 4.** Splitting observations for station NUKU. The splitting parameters are plotted as vectors at the event location. The station is shown as a triangle. The depths of the events (in kilometers) are also annotated.

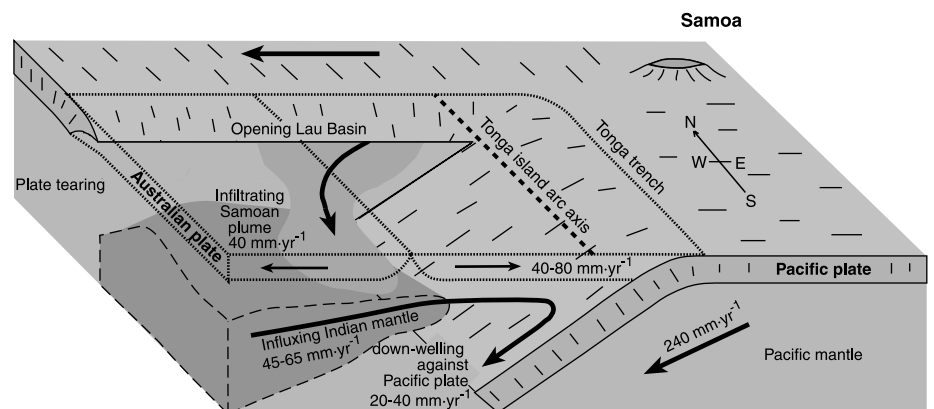
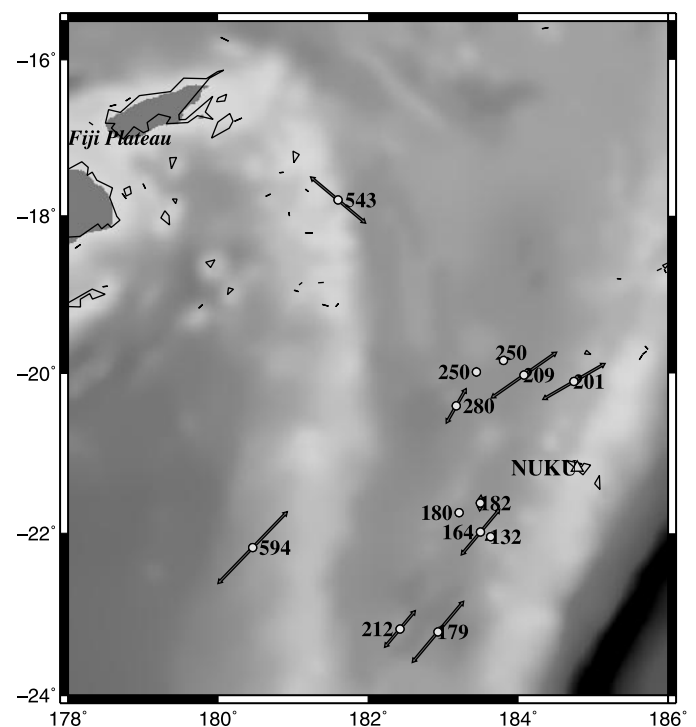


**Fig. 5.** After (38). Helium isotope data suggest southward flow of shallow mantle into the Lau basin through a tear in the subducted plate.

forearc and subvertical realignment in the wedge. However, their modeling did not include both slab dip and plate rollback, thus preventing direct comparison to the Tonga backarc. There is, however, geochemical evidence to suggest that along-arc mantle flow is occurring in this area. A change in Fiji magmatism from arc-like to ocean island basalt was attributed to influx of the Samoan Plume around 3 million years ago (35). A similar explanation for high Nb relative to other high-field-strength elements in lavas at the islands Tafahi and Niuatoputapu at the northern end of the Tonga-Kermadec subduction zone was also proposed (36). In addition, helium isotope data suggest flow of the Samoan Plume magma toward the Peggy Ridge at the northern end of the Lau basin (37). Later mapping by Turner and Hawkesworth (38) mapped the presence of these high  $^3\text{He}:$  $^4\text{He}$  further south into the Lau backarc. Such isotope signatures, which are characteristic of the Samoan Plume, may be evidence of the flow of shallow mantle (38) from the Samoan Plume into the Lau basin, parallel to the trench, through a tear in the subducting Pacific plate (Fig. 5). These results match both the geographical locations of our stations and the azimuth of mantle flow we would infer from our anisotropy observations. We infer, therefore, that the observations of along-arc fast anisotropy axes reflect this geochemical mapping of along-arc mantle flow and are probably resulting from slab rollback and the along-strike component of the absolute plate motions.

References and Notes

1. Seismic anisotropy is the phenomenon in which the velocity of a seismic wave through a medium depends on the wave's polarization or propagation direction.
2. N. I. Christensen, *Geophys. J. R. Astron. Soc.* **76**, 89 (1984).
3. S. Zhang, S. Karato, *Nature* **375**, 774 (1995).
4. A. Tommasi, *Earth Planet. Sci. Lett.* **160**, 1 (1998).
5. M. Bystricky, K. Kunze, L. Burlini, J. P. Burg, *Science* **290**, 1564 (2000).
6. N. M. Ribe, *J. Geophys. Res.* **94**, 4213 (1989).
7. M. K. Savage, *Rev. Geophys.* **37**, 65 (1999).
8. D. McKenzie, *Geophys. J. R. Astron. Soc.* **58**, 689 (1979).
9. J. R. Bowman, M. Ando, *Geophys. J. R. Astron. Soc.* **88**, 25 (1987).
10. K. M. Fischer, D. A. Wiens, *Earth Planet. Sci. Lett.* **142**, 253 (1996).
11. M. J. Fouch, K. M. Fischer, *J. Geophys. Res.* **101**, 15987 (1996).
12. K. M. Fischer, M. J. Fouch, D. A. Wiens, M. S. Boettcher, *Pure Appl. Geophys.* **151**, 463 (1998).
13. C. E. Hall, K. M. Fischer, E. M. Parmentier, *J. Geophys. Res.* **105**, 28009 (2000).
14. E. a. J. N. Sandvol, *J. Geophys. Res.* **102**, 9911 (1997).
15. W. Alvarez, *J. Geophys. Res.* **87**, 6697 (1982).
16. R. M. Russo, P. G. Silver, *Nature* **263**, 1105 (1994).
17. K. Gledhill, D. Gubbins, *Phys. Earth Planet. Int.* **95**, 227 (1996).
18. V. Peyton et al., *Geophys. Res. Lett.* **28**, 379 (2001).
19. J. Buttles, P. Olson, *Earth Planet. Sci. Lett.* **164**, 245 (1998).
20. K. M. Fischer, M. Parmentier, A. R. Stine, E. R. Wolf, in preparation.
21. D. K. Blackman et al., *Geophys. J. Int.* **127**, 415 (1996).

22. H. H. Hess, *Nature* **203**, 629 (1964).
23. C. J. Wolfe, S. C. Solomon, D. R. Toomey, D. W. Forsyth, *Eos* **77**, F653 (1996).
24. C. J. Wolfe, P. G. Silver, *J. Geophys. Res.* **103**, 749 (1998).
25. I. T. Bjarnason, C. J. Wolfe, S. C. Solomon, G. Gudmundson, *Geophys. Res. Lett.* **23**, 459 (1996).
26. D. W. Forsyth, S. C. Webb, L. M. Dorman, Y. Shen, *Science* **280**, 1235 (1998).
27. Seismic instruments are composed of three orthogonal components: one vertical and two horizontal. Land stations are normally oriented so that one horizontal component is east-west and the other is north-south. OBS instruments are not emplaced by hand, and so the orientations of the horizontal components are not known a priori.
28. E. A. Flinn, *Proc. IEEE* **53**, 1874 (1965).
29. S-wave splitting is the observation of two S-wave arrivals with orthogonal polarization due to anisotropy. The splitting time is the time between the

- arrivals. The fast azimuth corresponds to the polarization azimuth of the first arriving S wave.
30. P. N. Chopra, M. S. Paterson, *J. Geophys. Res.* **89**, 7861 (1984).
31. H. Jung, K.-H. Lee, S.-i. Karato, *Eos* **81**, S53 (2000).
32. J.-M. Kendall, *Geophys. Res. Lett.* **21**, 301 (1994).
33. M. E. Zimmerman, S. Zhang, D. L. Kohlstedt, S. Karato, *Geophys. Res. Lett.* **26**, 1505 (1999).
34. M. J. Fouch, K. M. Fischer, *Geophys. Res. Lett.* **25**, 1221 (1998).
35. J. Gill, P. Whelan, *J. Geophys. Res.* **94**, 4579 (1989).
36. J. I. Wendt, M. Regelous, K. D. Collerson, A. Ewart, *Geology* **25**, 611 (1997).
37. R. J. Poreda, H. Craig, *Earth Planet. Sci. Lett.* **113**, 487 (1992).
38. S. Turner, C. Hawkesworth, *Geology* **26**, 1019 (1998).
39. M. Bevis et al., *Nature* **374**, 249 (1995).
40. A. E. Gripp, R. G. Gordon, *Geophys. Res. Lett.* **17**, 1107 (1990).

3 January 2001; accepted 19 March 2001

## Detection of Widespread Fluids in the Tibetan Crust by Magnetotelluric Studies

Wenbo Wei,<sup>1</sup> Martyn Unsworth,<sup>2\*</sup> Alan Jones,<sup>3</sup> John Booker,<sup>4</sup>  
Handong Tan,<sup>1</sup> Doug Nelson,<sup>5</sup> Leshou Chen,<sup>1</sup> Shenghui Li,<sup>4</sup>  
Kurt Solon,<sup>5</sup> Paul Bedrosian,<sup>4</sup> Sheng Jin,<sup>1</sup> Ming Deng,<sup>1</sup>  
Juanjo Ledo,<sup>3</sup> David Kay,<sup>4</sup> Brian Roberts<sup>3</sup>

Magnetotelluric exploration has shown that the middle and lower crust is anomalously conductive across most of the north-to-south width of the Tibetan plateau. The integrated conductivity (conductance) of the Tibetan crust ranges from 3000 to greater than 20,000 siemens. In contrast, stable continental regions typically exhibit conductances from 20 to 1000 siemens, averaging 100 siemens. Such pervasively high conductance suggests that partial melt and/or aqueous fluids are widespread within the Tibetan crust. In southern Tibet, the high-conductivity layer is at a depth of 15 to 20 kilometers and is probably due to partial melt and aqueous fluids in the crust. In northern Tibet, the conductive layer is at 30 to 40 kilometers and is due to partial melting. Zones of fluid may represent weaker areas that could accommodate deformation and lower crustal flow.

The Tibetan plateau is the largest area of thickened and elevated continental crust on Earth and a direct consequence of the ongoing India-Asia collision (1). Knowledge of the structure and evolution of the plateau has advanced through modern geophysical studies that began in the 1980s with a Sino-French collaboration. Magnetotelluric (MT) data collected during this project detected unusually high electrical conductivity in the crust of southern Tibet (2). In combination with elevated heat flow (3), this was attribut-

ed to the presence of partial melt at shallow depths in the crust. In 1995, Project INDEPTH (4) acquired MT data in southern Tibet with the use of more advanced instrumentation and data-processing techniques (Fig. 1) (5). These data confirmed the existence of a high-conductivity zone at a depth of 15 to 20 km in southern Tibet that was coincident with seismic bright spots and a seismic low-velocity zone (6–8). These observations gave additional support to the idea that the high-conductivity layer represents partial melt in the Tibetan crust (9).

However, both of these MT surveys (2, 5) were located within the Yadong-Gulu rift, one of the north-south-trending rifts that accommodate the ongoing east-west extension in southern Tibet (10). To determine if the conductive crust was limited to the rifts, we collected additional MT data in 1998 and 1999 (500 and 600 lines, Fig. 1). A charac-

<sup>1</sup>Department of Applied Geophysics, China University of Geosciences, Beijing, People's Republic of China. <sup>2</sup>Institute of Geophysical Research, University of Alberta, Edmonton, Alberta T6G 2J1, Canada. <sup>3</sup>Geological Survey of Canada, Ottawa, Canada. <sup>4</sup>Geophysics Program, University of Washington, Seattle, WA 98195, USA. <sup>5</sup>Geological Sciences, Syracuse University, Syracuse, NY 13244, USA.

\*To whom correspondence should be addressed.